Journal of Power Sources 195 (2010) 614–620

Contents lists available at ScienceDirect

Journal of Power Sources

journal homepage: www.elsevier.com/locate/jpowsour

Gamma ray degradation of electrolytes containing alkylcarbonate solvents and a lithium salt

Magaly Caillon-Caravanier[a,*], Jennifer Jones[a], Mérièm Anouti[a], Frédéric Montigny[b], Patrick Willmann[c], Jean-Pierre David[d], Sabine Soonckindt[d], Daniel Lemordant[a]

[a] Laboratoire CIME/PCMB (EA4244), Université F. Rabelais, Faculté des Sciences et Techniques, Parc de Grandmont, 37200 Tours, France
[b] Plateau d'Analyse Chimique, Université F. Rabelais, Faculté de Pharmacie, 31 avenue Monge 37200 Tours, France
[c] CNES, 18 avenue E. Belin, 31055 Toulouse, France
[d] Département Environnement Spatial DSEP/ONERA, 2, avenue E. Belin, 31055 Toulouse, France

ARTICLE INFO

Article history:
Received 27 January 2009
Received in revised form 30 June 2009
Accepted 9 July 2009
Available online 18 July 2009

Keywords:
Gamma irradiation
Electrolyte
Vinylene carbonate
Polymerization
Lithium-ion
Lithium hexafluorophosphate

ABSTRACT

Lithium-ion batteries for space applications, such as satellites, are subjected to cosmic radiations, in particular, γ-irradiation. In this study, the effects of this radiation on electrolytes and their components used in the lithium-ion batteries are investigated. The conductivity and viscosity of the samples have been measured before and after the irradiation. The modifications are evaluated by spectral analyses such as Fourier transform infrared spectroscopy (FTIR), nuclear magnetic resonance spectroscopy (^{1}H and ^{13}C NMR), solid phase microextraction-gas chromatography (SPME-GC) and gas chromatography–mass spectroscopy (GC–MS). The experimental results show that only the samples containing vinylene carbonate and/or the lithium salt $LiPF_6$ are degraded by γ-radiation.

1. Introduction

Batteries used to store energy on board of space vehicles must fulfil severe requirements: high energy density, long term cycling, high charge efficiency, low self-discharge [1,2]. This is especially true in the case of recent high power (above 10 kW) long life (10–15 years) geostationary satellites where the battery's weight may represent up to 10% that of the satellite making it the heaviest satellite's component. Considering the potential advantages of the lithium-ion technologies for space missions, CNES, ESA and SAFT have initiated in 1996 a program aiming to develop and fly a space lithium-ion battery on an experimental program. This battery, the pathfinder for lithium-ion in space, was launched on board of SMART I on September 27, 2003 and flew successfully during the 3 years of the mission. Since then, lithium-ion batteries have demonstrated on several spacecrafts their ability to fit at best space requirements and are therefore today considered as the baseline solution for geostationary satellite [3]. As all space equipments, batteries are subjected to radiations during their life in orbit so the effect of γ-rays on them has to be considered [4]. With the previous generation of alkaline space batteries (nickel–cadmium, nickel–hydrogen) this aspect was of limited concern as they use aqueous electrolytes and thick steel containers acting as radiation shields. This is not, of course, the case with lithium-ion technology which uses organic electrolytes and thin aluminium containers therefore it is now of vital importance to investigate effects of radiations on the battery's components.

The behavior of commercial Li-ion cells with $LiCoO_2$ and graphite as electrode materials in the presence of γ-rays has already been investigated [5,6]. Experimental results indicate that the cell performances are substantially deteriorated owing to radiation-induced defects in $LiCoO_2$ and production of carboxyl radicals [5] in the electrolyte. The radiation effects on $LiCoO_2$ active material have been reported recently [6]. It is found that the exposure to radiations results in a change in the cobalt valence, an extent of the Li–Co cation occupancy exchange and a decrease in the electrochemical capacity.

The aim of the present work is to investigate the effect of γ-rays on the electrolyte as a whole and on the different solvents and additives used in the formulation of the electrolyte: ethylene carbonate (EC), propylene carbonate (PC), γ-butyrolactone (GBL), dimethyl carbonate (DMC), diethyl carbonate (DEC), methyl butyrate (MB), ethyl acetate (EA), and vinylene carbonate (VC). All these components have been characterised before and after irradiation by ^{1}H

* Corresponding author. Tel.: +33 247366954; fax: +33 247367073.
E-mail address: magaly.caravanier@univ-tours.fr (M. Caillon-Caravanier).

0378-7753/$ – see front matter © 2009 Elsevier B.V. All rights reserved.
doi:10.1016/j.jpowsour.2009.07.015

and ^{13}C NMR, IR, GC–MS and SPME/GC–MS. Electrolyte mixtures (PC/EC/DMC, EC/DEC, EC/BL), containing $LiPF_6$ or $LiBF_4$ and VC (or not), have been characterised by their viscosities and conductivities before and after irradiation. All samples have been exposed to a 20 kGy (2 Mrad) total dose but using two different dose rates: 7.9 Gy h^{-1} (high rate, HR) during 107 days and 1.6 Gy h^{-1} (low rate, LR) during 523 days in order to investigate the influence of the dose rate on the degradation of the electrolyte molecules.

2. Experimental

2.1. Materials

Solvents: ethylene carbonate (EC), propylene carbonate (PC), dimethyl carbonate (DMC), diethyl carbonate (DEC), γ-byturolactone (BL), methyl butyrate (MB), and ethyl acetate (EA) are purchased from Aldrich (anhydrous 99.5%) and are used as received without further purification. Lithium salts: lithium hexafluorophosphate ($LiPF_6$) and lithium tetrafluoroborate ($LiBF_4$) are obtained from Aldrich and could be used as received (battery grade, ≥99.99%). The preparation of all the solutions is performed in dry-box atmosphere containing less than 0.1 ppm H_2O (MBraun Unilab).

Tables 1a and 1b detail the composition and constitution of samples studied in our work, along with their classification. Each sample is divided into three batches: the first is the control sample (quoted T), the second is exposed to a high irradiation dose (7.9 Gy h^{-1}, quoted as HR) during 107 days and the third is exposed to a low irradiation dose (1.6 Gy h^{-1}, quoted as LR) during 523 days. The batches HR and LR received the same total dose: 20 kGy.

Irradiation has been carried out in a dedicated room, equipped with a ^{60}Co source. This type of source produces 1.17 and 1.33 MeV gamma rays that are able to deposit ionizing energy homogeneously on thick samples. Gamma rays generate secondary electrons that lost their energy mainly in ionizing processes: this means that the ionizing dose is in fact deposited by electrons. The irradiation room is underground and thus is naturally thermally regulated at 19 ± 2 °C over long periods of time. The irradiation room has been fully characterised by a TLD dosimetry. At every time, radioactive activity decay of the source is taken into account to calculate the dose rates; furthermore, dose rates are periodically controlled with an ionization chamber dosimeter of the type "RADCAL 2026C".

2.2. Measurements

Ionic conductivities are measured using a Crison (GLP 31) digital conductimeter operating at variable frequencies associated with a conductivity cell Crison 52-92 equipped with platinum electrodes covered by black platinum (cell constant: 1 cm^{-1}). Measures were obtained with accuracy of 0.01 μS cm^{-1}. The temperature, fixed at 25 °C, is regulated by a JULABO thermostated bath. Viscosities are measured using a TA instrument rheometer (AR 1000) with conical geometry at 25 °C, with accuracy of 0.01 mPa s.

Samples composition is analyzed by Fourier transform infrared spectroscopy (FTIR) before and after irradiation. All infrared spectra are obtained from samples cast into a NaCl plate using a Brucker EQUINOX 55 FTIR. In the case of solid samples, a KBr plate was made with a press (Specac).

^{1}H and ^{13}C NMR spectra were recorded in $CDCl_3$ at room temperature on a Bruker Advance DPX 200 spectrometer using 5 mm sample tubes. Proton and carbon resonances were referenced internally to tetramethylsilane (TMS).

GC–MS instrumentation consisted of a Hewlett-Packard system (HP 5890 series II GC with an HP 5989A quadrupole MS). A Vf-5MS 25-m × 0.25-mm × 0.25-μm capillary column and a helium (99.99%) carrier gas at a flow rate of 1 mL min^{-1} were used. The injector temperature was maintained at 250 °C, and all injections were made in splitless mode. The GC oven was held at 50 °C for 1 min and then programmed to 250 °C at 10 °C min^{-1} and maintained for 10 min. The GC–MS transfer line was maintained at 280 °C, electron ionization at 70 eV, and the mass spectrum scanned from m/z 35–450. Chromatographic data were acquired using HP Chemstation software.

Table 1a
Solvent samples: composition and classification.

Pure solvents		
Solvents	Dose	$N^{\#}$
PC	HR	1
	LR	2
	T	3
DMC	HR	7
	LR	8
	T	9
DEC	HR	10
	LR	11
	T	12
BL	HR	13
	LR	14
	T	15
MB	HR	25
	LR	26
	T	27
EA	HR	28
	LR	29
	T	30

Solvent mixtures		
Solvent mixtures (v/v)	Dose	$N^{\#}$
EC/DMC (90/10)	HR	4
	LR	5
	T	6
PC/EC/DMC (20/20/60)	LR	66
	T	67
EC/DEC (40/60)	LR	68
	T	69
EC/BL (18/82)	LR	70
	T	71

Solvent mixtures with an additive			
Solvents	Additive (wt.% VC)	Dose	$N^{\#}$
DMC	2	HR	16
		LR	17
		T	18
	10	HR	19
		LR	20
		T	21
	20	HR	22
		LR	23
		T	24
PC/EC/DMC (20/20/60)	1	HR	31
		LR	32
		T	33
EC/DEC (40/60)	1	HR	34
		LR	35
		T	36
EC/BL (18/82)	1	HR	37
		LR	38
		T	39

Table 1b
Electrolyte samples: composition and classification.

Solvent mixtures (volume ratio)	Salt	Additive (wt.% VC)	Dose	$N^{\#}$
PC/EC/DMC (20/20/60)	$LiPF_6$ 1 M	1	HR	40
			LR	41
			T	42
EC/DEC (40/60)	$LiPF_6$ 1 M	1	HR	43
			LR	44
			T	45
EC/BL (18/82)	$LiBF_4$ 1 M	1	HR	46
			LR	47
			T	48
PC/EC/DMC (20/20/60)	$LiPF_6$ 1 M	None	HR	49
			LR	50
			T	51
EC/BL (18/82)	$LiBF_4$ 1 M	None	HR	64
			T	65

3. Results and characterisations

3.1. Visual investigation

The batches HR, LR and T are visually compared. All pure solvents and their mixtures remain transparent whatever the nature of the treatment. Solvent mixtures containing 1% by weight of VC are translucent and are apparently not modified by γ-irradiation. Nevertheless, solvent mixtures containing DMC show the appearance of a white trouble. This suspension thickens with increasing VC. These observations can be explained by the polymerization of VC into poly-VC under the effect of γ-radiation. As a matter of fact, the formation of oligomers by polymerization of VC was already demonstrated by several groups [7–9]. Ding et al. prepared the poly-VC by thermal polymerization with AIBN as an initiator [7]. Moreover, according to our observations the presence of DMC seems to promote this phenomenon.

After irradiation, the electrolyte solutions containing the $LiPF_6$ as lithium salt show a discoloration from straw brown to dark brown. This color change was also observed by Ding et al. [5] for an electrolyte EC/DEC/$LiPF_6$. Moreover, we can note that the discoloration is more strongly pronounced for HR batches. On the contrary, the electrolyte containing the $LiBF_4$ salt shows very little discoloration. The absence of precipitate in samples containing DMC and VC can be explained by the presence of ionic charges resulting from the dissociation of the lithium salt which prevent the formation of large polymers. Indeed, the ions in solution, act as radicals traps which stop the polymerization process and cause the formation of oligomers, which are not visible. Taking into account this result, we have tested the thermal stability of two samples of each electrolyte (PC/EC/DMC $LiPF_6$ 1 M and EC/BL $LiBF_4$ 1 M), one freshly prepared in a dry-box and another corresponding to the T batch. The experimentation is performed in a thermostated oven at 80 °C and 100 °C for samples 42, 48, 51 and 65 and for freshly prepared samples with the same composition (noted (A) for solution PC/EC/DMC $LiPF_6$ 1 M and (B) for mixture EC/BL $LiBF_4$ 1 M). The visual aspect is checked every hour and the results obtained are listed in Table 2. The discoloration observed for the $LiPF_6$-containing electrolyte at 80 °C is strongly pronounced while the samples containing $LiBF_4$ remain transparent. Several authors have shown that $LiPF_6$ is thermally unstable, inducing a discoloration of solutions [9–12]. This phenomenon is probably due to the formation of radicals [5].

3.2. Conductivity and viscosity measurements

Conductivity and viscosity of the samples measured at 25 °C are comparable for T, HR and LR batches. Table 3 indicates σ and η values for DMC samples and electrolytes solutions with $LiPF_6$ and $LiBF_4$ salts. For DMC and DMC + 2 wt.% VC, the variation in conductivity is very low and in the range of the instrument accuracy. For DMC + 10 and 20 wt.% VC, we can note a slight decrease in σ for HR and LR batches compared to the T batch. The same observation can be made for electrolytes containing VC compound. Indeed, in the samples containing DMC and VC, we have observed the polymerization of the VC compound. We can suppose that during the polymerization process, the impurities are trapped in the macromolecules formed. The higher conductivity obtained for the T batches with increasing VC content can be explained by impurities in VC or by the presence of free radicals. It can be concluded that the irradiation process does not involve the formation of ionic compounds.

The viscosity values show an increasing tendency for batches HR and LR. The high viscosity for sample 20 is due to the formation of the white solid (poly-VC) which thickens the solution.

Table 2
Color of PC/EC/DMC $LiPF_6$ (1 M) and EC/BL $LiBF_4$ (1 M) solutions with time and temperature.

$N^{\#}$	Temperature (°C)	Time (h)	Color of solution
A	80	30	Brown
B	80	30	Colorless
42	80	30	Brown
48	80	30	Colorless
51	80	30	Brown
65	80	30	Colorless
A	100	10	Dark brown
B	100	10	Colorless
42	100	10	Dark brown
48	100	10	Colorless
51	100	10	Dark brown
65	100	10	Colorless

3.3. Spectroscopy analyses

The FTIR spectra of all samples are measured before and after γ-radiation. In Fig. 1 are displayed for a comparison purpose, the

Table 3
σ and η at 25 °C for selected samples.

Designation	$N^{\#}$	$\sigma \pm 10^{-4}$ (mS cm^{-1})	$\eta \pm 0.01$ (mPa s)
DMC	7	[a]	0.57
	8	[a]	0.41
	9	[a]	0.52
DMC + 2 wt.% VC	16	[a]	0.78
	17	[a]	0.85
	18	[a]	0.70
DMC + 10 wt.% VC	19	0.00098	0.93
	20	0.00004	1.44
	21	0.00248	0.87
DMC + 20 wt.% VC	22	0.00005	0.85
	23	0.00015	0.96
	24	0.01563	0.93
PC/EC/DMC $LiPF_6$ + 1 wt.% VC	40	10.56	3.91
	41	10.71	3.60
	42	11.11	3.18
EC/BL $LiBF_4$ + 1 wt.% VC	46	7.14	4.40
	47	7.04	4.43
	48	7.89	4.15
PC/EC/DMC $LiPF_6$	49	11.47	3.80
	50	11.46	3.80
	51	11.38	2.92
EC/BL $LiBF_4$	64	7.47	4.36
	65	7.67	4.25

[a] Values lower than the detection limit of this apparatus.

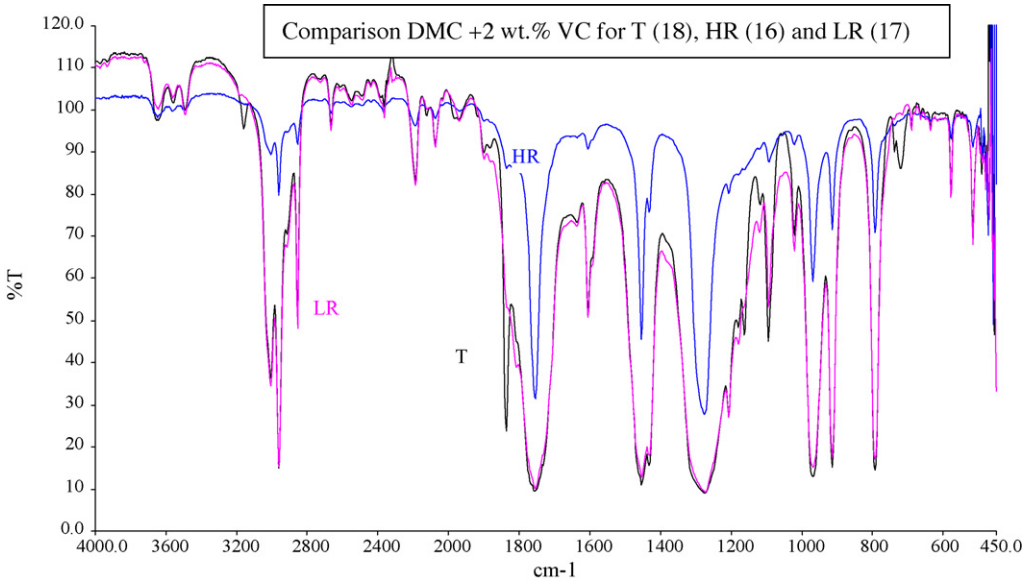

Fig. 1. Comparison of FTIR spectra of DMC + 2 wt.% VC mixtures according to the nature of the treatment.

FTIR spectra of DMC samples containing 2 wt.% VC for batches T, HR and LR. The pronounced peaks at 2800–3200 cm^{-1} attributed to the C–H symmetric stretching vibration in the vinylene group are considerably reduced after high rate irradiation [13]. The same observation is obtained for the peak at 1630 cm^{-1} assigned to the C=C stretching vibration of VC. This indicates that the sample placed near the radiation source is more strongly degraded than the sample exposed to the low rate dose. Another peak at about 1850 cm^{-1} attributed to $\upsilon_{C=O}$ of VC is only detected for the T batch. As observed previously, this result shows that in the DMC/VC solutions, it is the VC compound which is modified by γ-radiation.

In order to obtain information on the effect of the VC compound in the electrolyte, FTIR spectra of the samples containing 2, 10 and 20 wt.% VC are compared in Fig. 2 for HR batches. The bands at 3160 cm^{-1}, 1850 cm^{-1} and 1060–1160 cm^{-1} attributed to VC are absent in the DMC + 2 wt.% VC spectrum, whereas they are visible on the DMC + 10 and 20 wt.% VC spectra. The spectral differences of the mixtures containing the VC compound are attributed to the possible polymerization of a fraction of the VC into poly-VC [14]. The samples containing 10 and 20 wt.% of VC show that part of the VC remains unmodified under the effect of γ-radiation. In contrast, for samples containing 2 wt.% VC (quantity used in classical Li-ion batteries electrolytes), all VC is transformed.

There is no peak detected in chromatograms obtained with GC–MS for non-irradiated and γ-irradiated samples. Because of high volatility of carbonates, these compounds are with the solvent front, and are not detected by mass spectrometer. However, the flat chromatograms indicate that there is no more other organic volatile compounds in the samples analyzed. We can conclude that there is no degradation product.

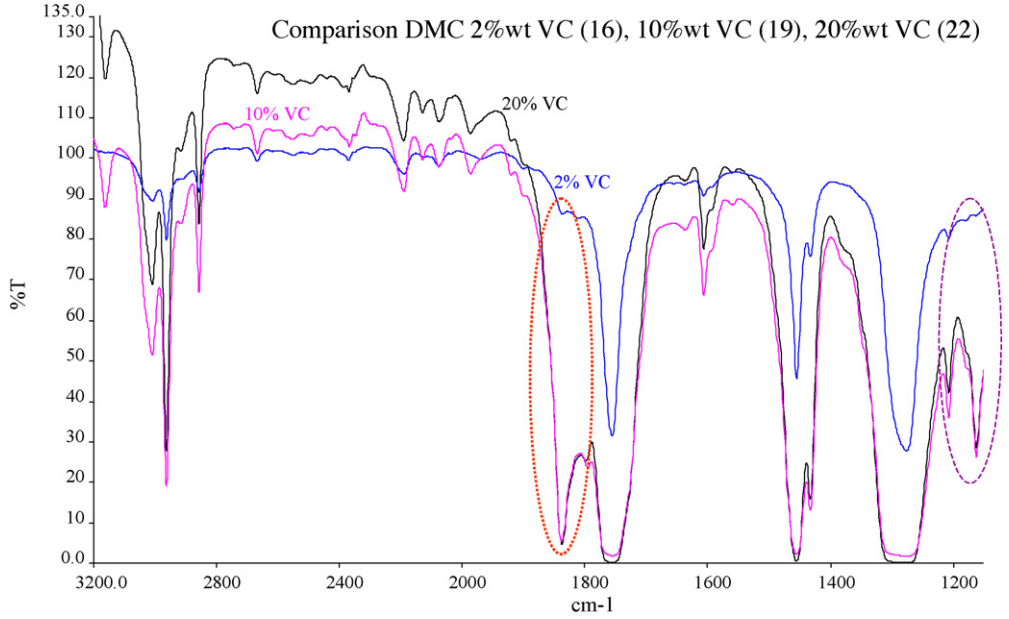

Fig. 2. Comparison of FTIR spectra of mixtures DMC + 2, 10 and 20 wt.% VC for HR batches.

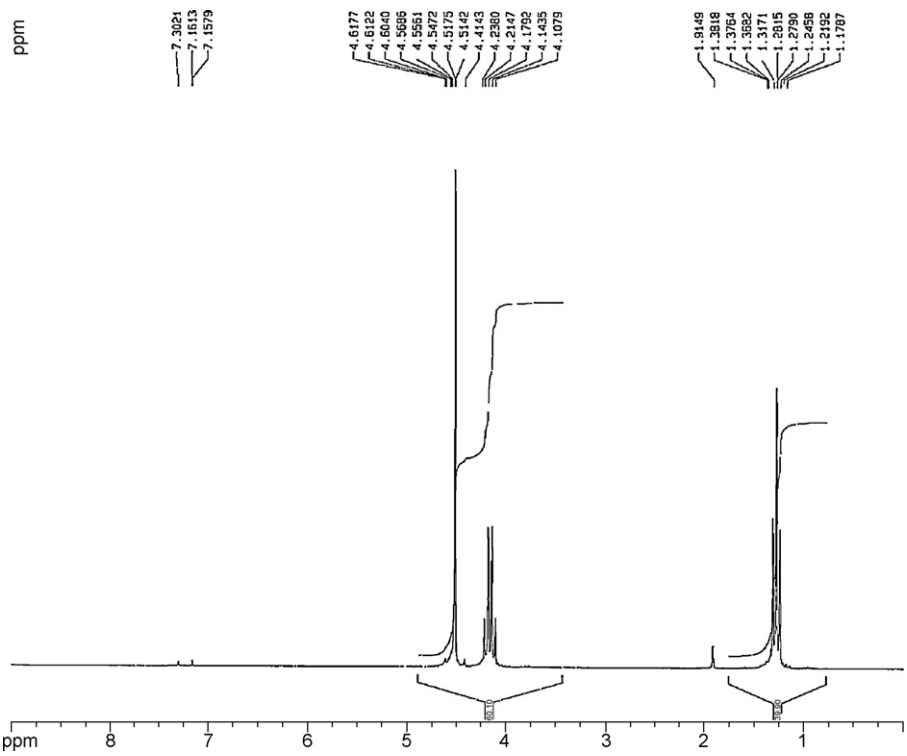

Fig. 3. ^{1}H NMR spectrum of EC/DEC + 1 wt.% VC (sample 36).

^{1}H and ^{13}C NMR experiments show that the only visible difference between these spectra consists in the disappearance of VC signals for γ-irradiated samples. As there is no other signals on these spectra, we must conclude that VC transforms into solid poly-VC. Fig. 3 shows the ^{1}H NMR spectrum of mixture 36 (EC/DEC + 1 wt.% VC). We can see on that spectrum the signal of VC ethylenic protons at 7.16 ppm. Fig. 4 shows the comparison of ^{1}H NMR spectra of mixtures 34 (up), 35 (middle) and 36 (down), in the 7.5–7 ppm region. We observe the total disappearance of VC signal during γ-irradiation. The 7.3 ppm peak is the solvent signal ($CDCl_3$). We have identical results with ^{13}C RMN spectra. Fig. 5 shows the spectrum of mixture number 36. The 132.3 ppm peak is attributed to VC carbonyl. The comparison of ^{13}C NMR spectra is presented in Fig. 6 for mixtures 34 (up), 35 (middle) and 36 (down), in the

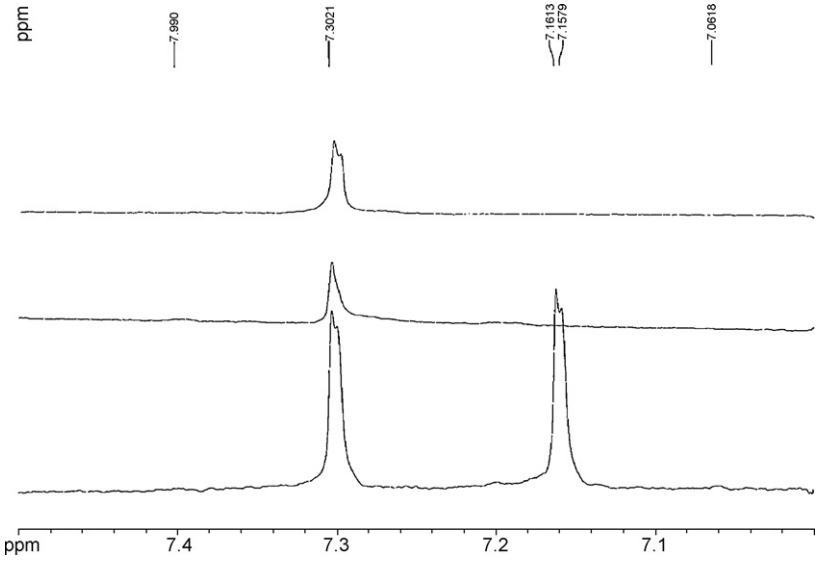

Fig. 4. Zoom of 7–7.5 ppm region for the spectrum of Fig. 6 showing VC signal at 7.16 ppm (bottom, sample 36), and disappearance of this signal for irradiated samples (middle, sample 35 and top, sample 34).

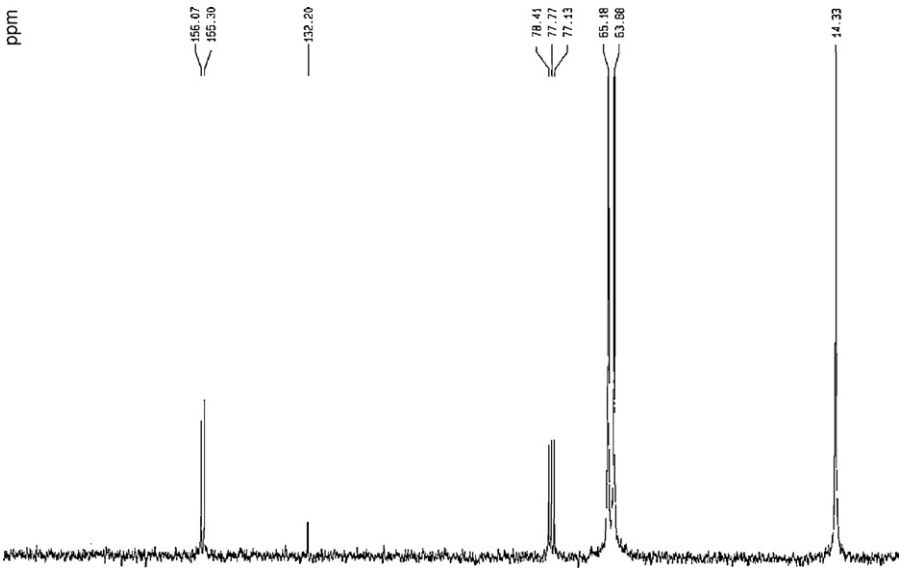

Fig. 5. ^{13}C NMR spectrum of the sample 36.

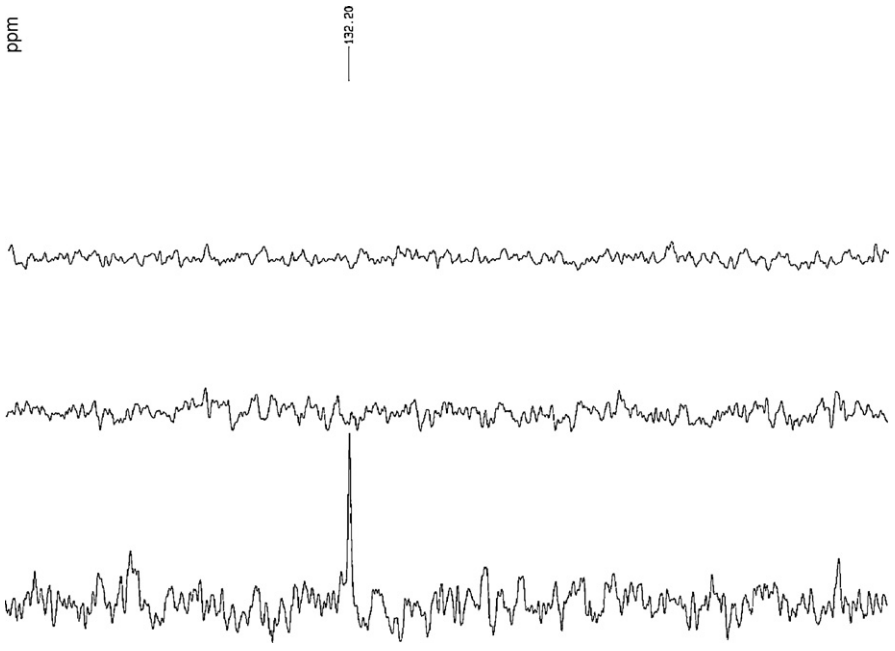

Fig. 6. ^{13}C NMR spectra for mixtures 34 (up), 35 (middle) and 36 (down), in the 140–120 ppm region.

140–120 ppm region showing disappearance of VC signal during γ-irradiation.

4. Conclusion

The investigation of the influence of γ-radiation on lithium-ion batteries is required for their optimization in space applications. This study is designed to investigate the effects of irradiation on the electrolyte and on its different components. It is shown that γ-radiations have a large impact only on VC as an electrolyte additive and on $LiPF_6$ as a lithium salt. In VC-containing samples, a great difference is noted before and after irradiation with the formation of a white solid in suspension. This phenomenon is particularly visible with other samples containing DMC. We attribute the formation of this solid to the low solubility of the polymeric species, mainly polycarbonate, in DMC which has a very low dielectric constant as compared to PC or EC. Several authors have described the polymerization reaction of the vinylene monomers [15,16]. Spectral studies indicate that the deterioration of VC is more pronounced for HR batches. The formation of macromolecules is visible in particular for DMC samples containing 10 wt.% and 20 wt.% of VC.

This paper also demonstrates that the electrolytes containing the lithium salt $LiPF_6$ are modified under a γ-radiation environment as the samples exposed to these radiations become colored as observed for heated $LiPF_6$ solutions. Consequently, γ-radiation induces the polymerization of VC into poly-VC (total or partial) and the degradation of $LiPF_6$ based electrolytes. At the opposite, the electrolytes containing $LiBF_4$ do not show any visible change. Hence, it would be preferable to use $LiBF_4$ instead of $LiPF_6$ in electrolytes designed for space applications and to replace VC by

another non-polymerizable additive to enhance the SEI transport properties.

References

[1] G. Gave, Y. Borthomieu, B. Lagattu, J.-P. Planchat, Acta Astronautica 54 (2004) 559.
[2] E.J. Plichta, M. Hendrickson, R. Thompson, G. Au, W.K. Behl, M.C. Smart, B.V. Ratnakumar, S. Surampudi, Journal of Power Sources 94 (2001) 160.
[3] Y. Borthomieu, B. Lagattu, S. Remy, J.-P. Semerie, Proc. of the 8th European Space Power Conference Constance Germany, September, 14–19, 2008.
[4] The natural space environment, effect on spacecraft, NASA RP-1350, November 1994.
[5] N. Ding, J. Zhu, Y.X. Yao, C.H. Chen, Electrochimica Acta 21 (2006) 6320.
[6] N. Ding, J. Zhu, Y.X. Yao, C.H. Chen, Chemical Physics Letters 426 (2006) 324.
[7] L. Ding, Y. Li, Y. Li, Y. Liang, European Polymer Journal 37 (2001) 2453.
[8] H. Ota, K. Shima, M. Ue, J.-I. Yamaki, Electrochimica Acta 49 (2004) 565.
[9] D. Aurbach, K. Gamolsky, B. Markovsky, Y. Gofer, M. Schmidt, U. Heider, Electrochimica Acta 47 (2002) 1423.
[10] Nagasubramanian, Journal of Power Sources 119–121 (2003) 811.
[11] H. Yang, G.V. Zhuang, P.N. Ross Jr., Journal of Power Sources 161 (2006) 573.
[12] J.S. Gnanaraj, E. Zinigrad, M.D. Levi, D. Aurbach, M. Smidt, Journal of Power Sources 119–121 (2003) 799.
[13] D. Autrey, A. del Rosario, J. Laane, Journal of Molecular Structure 550–551 (2000) 505.
[14] L. Chen, K. Wang, X. Xie, J. Xie, Journal of Power Sources 174 (2007) 538.
[15] H.J. Santner, K.-C. Möller, J. Ivanco, M.G. Ramsey, F.P. Netzer, S. Yamaguchi, J.O. Besenhard, M. Winter, Journal of Power Sources 119–121 (2003) 368.
[16] C. Korepp, H.J. Santner, T. Fujii, M. Ue, J.O. Besenhard, K.-C. Möller, M. Winter, Journal of Power Sources 158 (2006) 578.